Image Processing & Communications, vol. 20, no. 1, pp.5-12
DOI: 10.1515/ipc-2015-0025

DIGITAL IMAGE SEPARATION ALGORITHM BASED ON JOINT PDF OF MIXED IMAGES

MOHD WAJID MAYANK SHARMA

Department of Electronics and Communication Engineering,
Jaypee University of Information Technology, Solan 173234, India
wajidiitd@ieee.org,mayankwaknaghat@gmail.com

Abstract. In this article, we have presented an algorithm for separating the mixed or fused images. We have considered that the two independent histogram equalized digital images are linearly mixed, and the joint probability density function (PDF) or the scatter plot of the two observed or mixed images is used for separation. The objective and subjective separation results are presented, and observed to be better than the other existing techniques in terms of Peak signal-to-noise ratio (PSNR) and Signal-to-interference ratio (SIR).

1 Introduction

Separation of mixed and overlapped images is a frequently arising problem in image processing, for example separation of overlapped images obtained when photographing objects placed behind a glass window or windscreen, since most varieties of glass have semi-reflecting properties [2]. Reflections may create ambiguity in scene analysis, so there is a need to separate the desired and the reflected images from the superimposed or mixed images [16]. Mathematically, image mixture can be seen as

$$\boldsymbol{I} = \boldsymbol{AS} \tag{1}$$

$$\boldsymbol{A} = \begin{bmatrix} a_{11} & a_{12} \\ a_{21} & a_{22} \end{bmatrix} \tag{2}$$

where, $\boldsymbol{I} = [I_1\ I_2]^T$ are mixed images vector, $\boldsymbol{S} = [S_1\ S_2]^T$ are the original images vector and $\boldsymbol{A}$ is a mixing matrix. The observed images are weighted linear combination of source images and mixing weights are not known [18]. The mixed image separation is a blind source separation (BSS) problem, because neither source images, nor mixing coefficients are known. If we can estimate mixing matrix, the original unmixed images can also be estimated as

$$\boldsymbol{S} = \boldsymbol{A^{-1}I} \tag{3}$$

There are many other applications of source signal separation, namely image de-noising [1, 22], medical signal and image processing like FMRI, ECG, EEG, ultrasound images [17, 15, 21, 19], feature extraction in Content-

Based Image Retrieval (CBIR) [5, 6, 24], face recognition [6], compression redundancy reduction [11], watermarking [10, 13], remote sensing in cloud detection [7] where cloud detection of the atmospheric remote sensing image of a VHRR (very high resolution radiometer) is tested using separation technique, scientific data mining [20], finger print extraction for forensic use [4, 23].

The approaches for digital mixed image separation are scatter-plot based technique, principal component analysis (PCA), SVD-based ICA technique, etc. In scatter plot based technique, the geometrical shape of joint probability density function is used [9, 8, 12], for two histogram equalize mixed images the shape of joint pdf (or scatter plot) will be parallelogram [2, 3], and orientation of the parallelogram sides depends on mixing coefficients [3]. The robustness of this technique is high, if image sizes are large. The PCA based technique uses second order statistics of the observed images, it is a linear transformation that is derived from the second order signal statics (covariance structure). The ICA based technique uses higher order statistics provided that the observed images data is non-Gaussian and independent.

In this paper, it has been considered that the original images are histogram equalized and statistically independent, However, the automatic image separation procedure based on scatter data [8] of the observed images is established for the mixture of two images. The results are also compared with the SVD based ICA algorithm, where it has been assumed that maximum variance orientation is orthogonal to the minimum variance orientation [14]. The remaining paper is organized as follows. In section 2, the mixing procedure and the algorithm for image separation based on scatter plot is presented. In section 3, simulation setup and results are discussed and in section 4 results of scatter based technique are compared with SVD based ICA method. Section 5 concludes the paper.

2 Algorithm based on scatter data

When two histogram equalized images are linearly mixed as given in (4) and (5), then the observed images will no longer have uniform distributions

$$I_1 = a_{11}S_1 + a_{12}S_2 \tag{4}$$

$$I_2 = a_{21}S_1 + a_{22}S_2 \tag{5}$$

where a_{11}, a_{12}, a_{21}, and a_{22} are the mixing co-efficient and are required to be estimated along with the original images.

Let $f_{\boldsymbol{s_i^z}}(s_i^z)$ be the probability density function of the histogram equalized and zero-mean source images S_i^z,$i =$ 1 and 2 as given by (6)

$$f_{\boldsymbol{s_i^z}}(s_i^z) = \begin{cases} \frac{1}{2K}, & |s_i^z| \leq K \\ 0, & otherwise \end{cases} \tag{6}$$

where, K is the highest intensity value of the images S_i^z. Then the resultant distribution of the observed images $I_1$and I_2 for $a_{12} > a_{11}$ and $a_{22} > a_{21}$ is given in (7) and (8)

$$f_{\boldsymbol{w_1}}(w_1) = \begin{cases} \frac{1}{4a_{11}a_{12}K^2}(a_{11}K + a_{12}K + w_1), & -(a_{11}+a_{12})K \leq w_1 \leq -(a_{12}-a_{11})K \\ \frac{1}{2a_{12}K}, & -(a_{12}-a_{11})K \leq w_1 \leq (a_{12}-a_{11})K \\ \frac{1}{4a_{11}a_{12}K^2}(a_{11}K + a_{12}K - w_1), & (a_{12}-a_{11})K \leq w_1 \leq (a_{11}+a_{12})K \\ 0, & Otherwise \end{cases} \tag{7}$$

$$f_{w_2}(w_2) = \begin{cases} \frac{1}{4a_{21}a_{22}K^2}(a_{21}K + a_{22}K + w_2), & -(a_{21}+a_{22})K \le w_2 \le -(a_{22}-a_{21})K \\ \frac{1}{2a_{22}K}, & -(a_{22}-a_{21})K \le w_2 \le (a_{22}-a_{21})K \\ \frac{1}{4a_{21}a_{22}K^2}(a_{21}K + a_{22}K - w_2), & (a_{22}-a_{21})K \le w_2 \le (a_{21}+a_{22})K \\ 0, & Otherwise \end{cases} \tag{8}$$

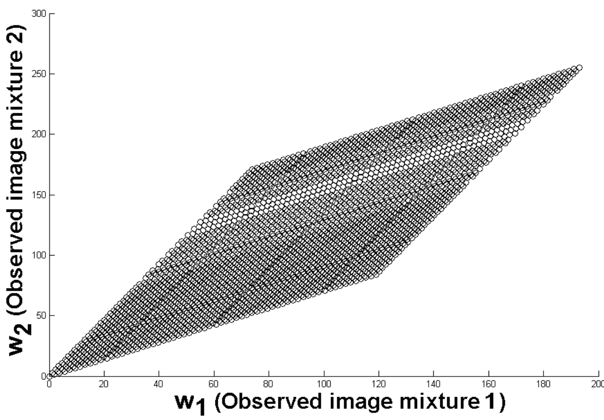

Fig. 1: Scatter plot for the two mixed images

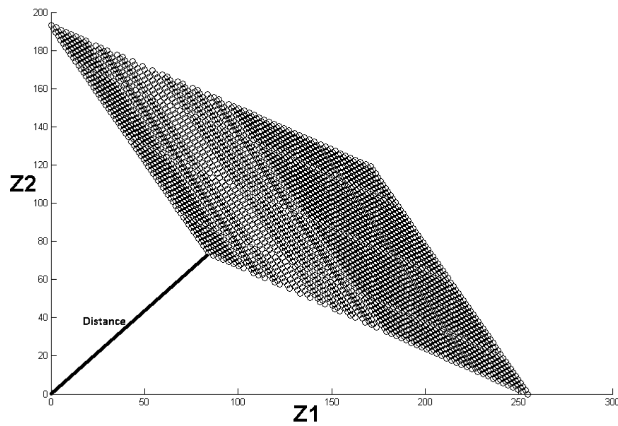

Fig. 2: Rotated (anti-clock wise by 90^o) scatter plot for the mixed images

where, w_1 and w_2 are the row vectors of order 1 by N^2 of the observed images I_1 and I_2. So the joint probability density function or scatter plot of the two observed images will be parallelogram in shape. The scatter data based image separation algorithm for the two mixed digital images I_1 and I_2 (order of N by N) is given in Algorithm 1.

The scatter plot of the two mixed images is shown in Fig. 1 and their rotated variants are given in figs. 2 and 3. Figure 2 is the anticlockwise rotated (by 90^o) plot of the original scatter plot given in Fig. 1, while Fig. 3 is the clockwise rotated (by 90^o) plot of the original scatter plot. Since, four vertices of the scatter plot contains the information of the mixing matrix, these variants of the scatter plot is used to estimate the four vertices in the given algorithm. In Fig. 2 and 3, the smallest distance between the origin and a point on the scatter plot is calculated as shown by the solid line in these figures. The point in a scatter plot corresponding to smallest distance have maximum probability to be a vertex point of a parallelogram.

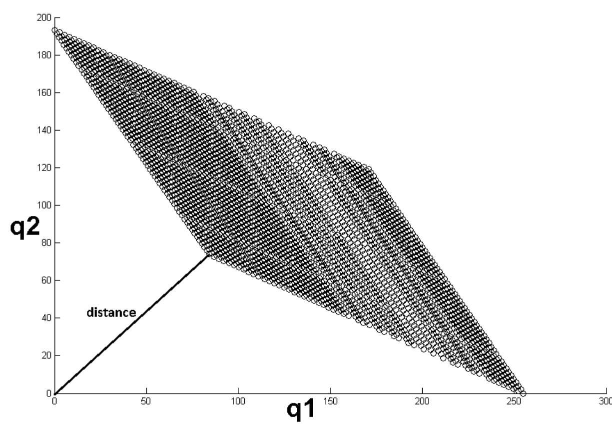

Fig. 3: Rotated (clockwise by 90^o) scatter plot

3 Simulation Setup and Results

For the image separation of mixed images, the given algorithm has been applied on 45 mixed image pairs and their performance is evaluated in terms of PSNR and sig-

Algorithm 1 Algorithm for image separation based on scatter plot

1. Find maximum and minimum values from I_1 and I_2 and consider that the four vertices of the parallelogram shaped scatter plot of images I_1 and I_2 are A, B, C and D.
   (a) $x_a = max(I_1)$ and $y_a = max(I_2)$
   (b) $x_c = min(I_1)$ and $y_c = min(I_2)$,

   where (x_a, y_a) and (x_c, y_c) are the co-ordinates of the two vertices A and C of the parallelogram.
2. Convert I_1 and I_2 in to row vectors
   (a) $w_1(1, (x-1) * N + y) = I_1(x, y)$
   (b) $w_2(1, (x-1) * N + y) = I_2(x, y)$

   where,w_1 and w_2 are the row vectors of order 1 by N^2
3. $Z = \begin{bmatrix} -w_2 \\ w_1 \end{bmatrix} - \begin{bmatrix} min(-w_2) \\ min(w_1) \end{bmatrix}$ is the anti-clockwise rotated (by 90^o) scattered data.
4. Find vector V , $V = \begin{bmatrix} ||z_1|| & ||z_2|| & \cdots & ||z_{N^2}|| \end{bmatrix}$, where $||z_p|| = \sqrt{Z^2(1,p) + Z^2(2,p)}$ is the distances of the points on the anti-clockwise rotated (by 90^o) scatter plots from the origin.
5. Search for the smallest component in the row vector V and store its index in j
6. $\begin{bmatrix} x_d \\ y_d \end{bmatrix} = \begin{bmatrix} Z(2,j) + min(w_1) \\ -Z(1,j) - min(-w_2) \end{bmatrix}$ is the estimated co-ordinated of the parallelogram vertex D.
7. $Q = \begin{bmatrix} w_2 \\ -w_1 \end{bmatrix} - \begin{bmatrix} min(w_2) \\ min(-w_1) \end{bmatrix}$ is the clockwise rotated (by 90^o) scattered data.
8. Find vector T, $T = \begin{bmatrix} ||q_1|| & ||q_2|| & \cdots & ||q_{N^2}|| \end{bmatrix}$, where $||q_p|| = \sqrt{Q^2(1,p) + Q^2(2,p)}$ is the distances of the points on the clockwise rotated (by 90^o) scatter plots from the origin.
9. Search for the smallest component in the row vector T and store its index in i
10. $\begin{bmatrix} x_b \\ y_b \end{bmatrix} = \begin{bmatrix} -Q(2,i) - min(-w_1) \\ Q(1,i) + min(w_2) \end{bmatrix}$ is the estimated co-ordinated of the parallelogram vertex B.
11. The estimated mixing matrix $\boldsymbol{A}$is given as, $\boldsymbol{A} = \frac{1}{2L}\begin{bmatrix} x_a + x_d & x_a - x_d \\ y_a - y_b & y_a + y_b \end{bmatrix}$, where L is the number of intensity levels in the given digital image.
12. The estimated images vector is $\boldsymbol{X} = \boldsymbol{A}^{-1}\begin{bmatrix} I_1 \\ I_2 \end{bmatrix}$
13. The reordering of $\boldsymbol{X}$ in to two images each of order NxN : if $mod(y, N) \neq 0$, then $q = mod(y, N)$; else $q = N$. So separated images $I_1^{separated}$ and $I_2^{separated}$ are given as, $I_1^{separated}(\lceil \frac{y}{N} \rceil, q) = \boldsymbol{X}(1, y)$ and $I_2^{separated}(\lceil \frac{y}{N} \rceil, q) = \boldsymbol{X}(2, y)$; which are the approximates of the original images $S_1 \approx I_1^{separated}$ & $S_2 \approx I_2^{separated}$.

Fig. 4: Original Images 'Ima1' and 'Ima2' (top row), mixed images (middle row) and separated images (last row) using scatter plot based technique.

nal to interference ratio (SIR). These fused images for $a_{11} = 0.467, a_{12} = 0.29, a_{21} = 0.33$, and $a_{22} = 0.67$ are generated using randomly chosen 10 images in the bitmap format with a resolution of 512×512 pixels. Few original images, mixed images and separated images are shown in Fig. 4 to 5.

4 Performance evaluation and comparison

The performance of the scatter based techniques with the presented algorithm is compared with SVD based ICA method. It can be observed from Fig. 6 and 7 that both PSNR and SIR for scatter based method is more than the

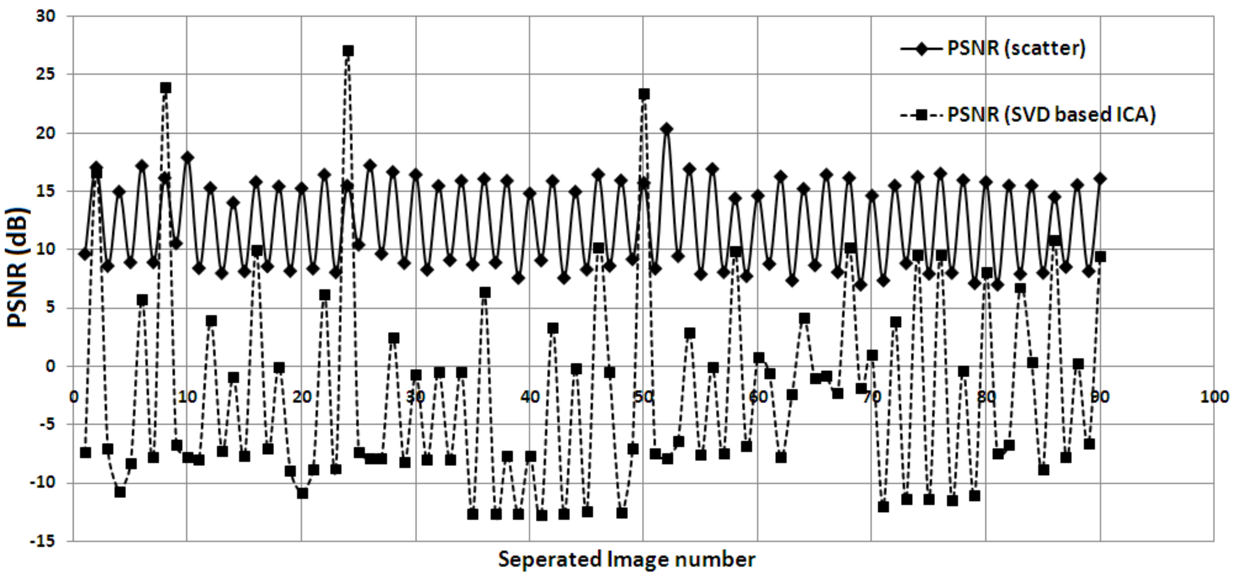

Fig. 6: PSNR for the separated images using scatter-plot based technique and SVD-based ICA techniques.

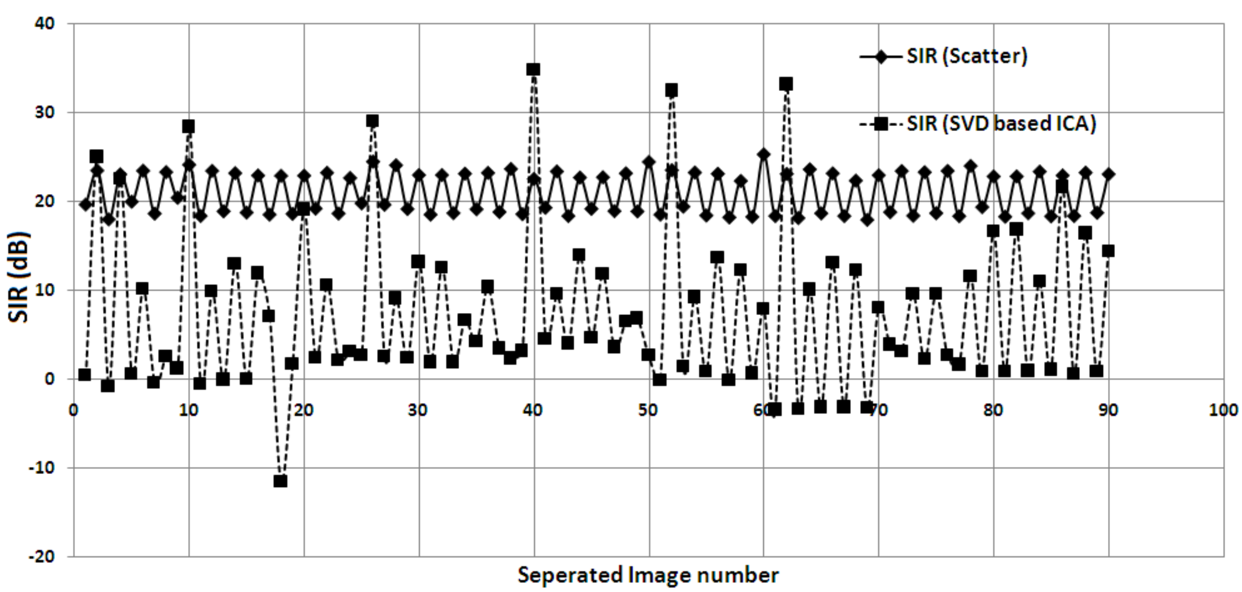

Fig. 7: SIR for the separated images using scatter-plot based technique and SVD-based ICA techniques.

Fig. 5: Original Images 'Ima3' and 'Ima4' (top row), mixed images (middle row) and separated images (last row) using scatter plot based technique.

Tab. 1: Percentage error in estimated mixing coefficient.

Mixing coefficients	Average percentage error
a_{11}	11.656 %
a_{12}	19.881 %
a_{21}	1.240 %
a_{22}	1.228 %

SVD based ICA method for all mixed image pairs separation. The average PSNR and average SIR for scatter based technique is more than 12 dB and 21 dB, respectively, while for SVD based ICA method average PSNR is around -2.5 dB and average SIR is 7.2 dB. Also, the average percentage error of mixing coefficient estimates for 45 mixtures is calculated and is given in Table 1.

5 Conclusion

The given algorithm for image separation based on scatter plot successfully separates the histogram equalized mixed images and performs better then SVD based ICA technique in terms of PSNR and SIR. We have tested this scatter-plot based algorithm on 45 mixed image pairs and estimated all four mixing co-coefficients along with the original unmixed images. Further, it has been observed that the average percentage errors in the estimated mixing co-efficients are different for different co-coefficients. The average (over 90 separated images) PSNR and average SIR for scatter based technique is more than 12 dB and 21 dB respectively, while for SVD based ICA method average PSNR is around -2.5 dB and average SIR is 7.2 dB. In this investigation, the robustness of the joint PDF based image separation technique is tested only for mixture of two images, so the future work may include the separation of three image mixture.

References

[1] Abbass, M.,Y., Shehata, S.,A., Haggag, S.,S., Diab, S.,M., Salam, B.,M., El-Rabaie, S., Abd El-Samie, F.,E. (2013). Blind separation of noisy images using finite Ridgelet Transform and wavelet de-noising. *In Electronics, Communications and Computers (JEC-ECC), 2013 Japan-Egypt International Conference on* (pp. 176-181). IEEE

[2] Bronstein, A.,M., Bronstein, M.,M., Zibulevsky, M., Zeevi, Y.,Y. (2005). Sparse ICA for blind separation of transmitted and reflected images. *International Journal of Imaging Systems and Technology*, 15(1), 84-91

[3] Carasso, D., Vizel, E., Zeevi, Y.,Y. (2009, July). Blind Source Separation using mixtures scatter plot properties. In *Digital Signal Processing, 2009 16th International Conference on* (pp. 1-6). IEEE

[4] Chen, F., Feng, J., Jain, A.,K., Zhou, J., Zhang, J. (2011). Separating overlapped fingerprints. *Information Forensics and Security, IEEE Transactions on*, 6(2), 346-359

[5] Choras, R.,S. (2007). Image feature extraction techniques and their applications for CBIR and biometrics systems. *International journal of biology and biomedical engineering*, 1(1), 6-16

[6] Hong, Z.,Q. (1991). Algebraic feature extraction of image for recognition. *Pattern recognition*, 24(3), 211-219

[7] Huadong, D., Yongqi, W., Yaming, C. (2009). Studies on Cloud Detection of Atmospheric Remote Sensing Image Using ICA Algorithm. In *Image and Signal Processing, 2009. CISP'09. 2nd International Congress on* (pp. 1-4). IEEE

[8] Hyvarinen, A. (2001). Blind source separation by nonstationarity of variance: a cumulant-based approach. *Neural Networks, IEEE Transactions on*, 12(6), 1471-1474

[9] Hyvarinen, A., Karhunen, J., Oja, E. (2004). *Independent component analysis* (Vol. 46). John Wiley & Sons

[10] Jadhav, S. D., Bhalchandra, A. S. (2010). Blind source separation based robust digital image watermarking using wavelet domain embedding. In *Cybernetics and Intelligent Systems (CIS), 2010 IEEE Conference on* (pp. 162-167). IEEE

[11] Koh, C. C., Mukherjee, J., Mitra, S. K. (2003). New efficient methods of image compression in digital cameras with color filter array. *Consumer Electronics, IEEE Transactions on*, 49(4), 1448-1456

[12] Kumari, M., Wajid, M. (2013). Source Separation of Independent Components. LRC, JUIT, 2013, SPR 621 KUM, SPM1327

[13] Kundur, D., Hatzinakos, D. (1997). A robust digital image watermarking scheme using the wavelet-based fusion. In *icip* (p. 544). IEEE

[14] Kutz, J.,N. (2013). *Data-driven modeling & scientific computation: methods for complex systems & big data.* Oxford University Press

[15] Parra, L., Sajda, P. (2003). Blind source separation via generalized eigenvalue decomposition. *The Journal of Machine Learning Research*, 4, 1261-1269

[16] Singh, D.,K., Tripathi, S., Kalra, P.,K. (2006). Separation of image mixture using complex ICA. *In The 9th Asian Symposium on Information Display ASID06*, 314-317

[17] Sternberg, S.,R. (1983). Biomedical image processing. *Computer*, 1(16), 22-34

[18] Tonazzini, A., Bedini, L., Salerno, E. (2006). A Markov model for blind image separation by a mean-field EM algorithm. *Image Processing, IEEE Transactions on*, 15(2), 473-482

[19] Virmani, J., Kumar, V., Kalra, N., Khandelwa, N. (2013). Pca-SVm based caD System for Focal liver lesions using B-mode ultrasound Images. *Defence Science Journal*, 63(5), 478-486

[20] Ye, N. (Ed.). (2003). *The handbook of data mining* (Vol. 24). Mahwah, NJ/London: Lawrence Erlbaum Associates, Publishers

[21] Zarzoso, V., Comon, P. (2008). Robust independent component analysis for blind source separation and extraction with application in electrocardiography. In *Engineering in Medicine and Biology Society, 2008. EMBS 2008. 30th Annual International Conference of the IEEE* (pp. 3344-3347). IEEE

[22] Zhang, L., Dong, W., Zhang, D., Shi, G. (2010). Two-stage image denoising by principal component analysis with local pixel grouping. *Pattern Recognition*, 43(4), 1531-1549

[23] Zhao, Q., Jain, A.,K. (2012). Model based separation of overlapping latent fingerprints. *Information Forensics and Security, IEEE Transactions on*, 7(3), 904-918

[24] Zou, W., Li, Y., Lo, K. C., Chi, Z. (2006). Improvement of image classification with wavelet and independent component analysis (ICA) based on a structured neural network. In *Neural Networks, 2006. IJCNN'06. International Joint Conference on* (pp. 3949-3954). IEEE